APPLIED AND ENVIRONMENTAL MICROBIOLOGY, Nov. 1997, p. 4272–4281 Vol. 63, No. 11
0099-2240/97/$04.00+0

Degradation of the Fluoroquinolone Enrofloxacin by the Brown Rot Fungus *Gloeophyllum striatum*: Identification of Metabolites

HEINZ-GEORG WETZSTEIN,[1]* NORBERT SCHMEER,[1] AND WOLFGANG KARL[2]

Animal Health Research[1] and Central Research,[2] Bayer AG, D-51368 Leverkusen, Germany

Received 9 December 1996/Accepted 22 August 1997

The degradation of enrofloxacin, a fluoroquinolone antibacterial drug used in veterinary medicine, was investigated with the brown rot fungus *Gloeophyllum striatum*. After 8 weeks, mycelia suspended in a defined liquid medium had produced 27.3, 18.5, and 6.7% $^{14}CO_2$ from [^{14}C]enrofloxacin labeled either at position C-2, at position C-4, or in the piperazinyl moiety, respectively. Enrofloxacin, applied at 10 ppm, was transformed into metabolites already after about 1 week. The most stable intermediates present in 2-day-old supernatants were analyzed by high-performance liquid chromatography combined with electrospray ionization mass spectrometry. Eight of 11 proposed molecular structures could be confirmed by ^{1}H nuclear magnetic resonance spectroscopy or by cochromatography with reference compounds. We identified (i) 3-, 6-, and 8-hydroxylated congeners of enrofloxacin, which have no or only very little residual antibacterial activity; (ii) 5,6- (or 6,8-), 5,8-, and 7,8-dihydroxylated congeners, which were prone to autoxidative transformation; (iii) an isatin-type compound as well as an anthranilic acid derivative, directly demonstrating cleavage of the heterocyclic core of enrofloxacin; and (iv) 1-ethylpiperazine, the 7-amino congener, and desethylene-enrofloxacin, representing both elimination and degradation of the piperazinyl moiety. The pattern of metabolites implies four principle routes of degradation which might be simultaneously employed. Each route, initiated by either oxidative decarboxylation, defluorination, hydroxylation at C-8, or oxidation of the piperazinyl moiety, may reflect an initial attack by hydroxyl radicals at a different site of the drug. During chemical degradation of [4-^{14}C]enrofloxacin with Fenton's reagent, five confirmatory metabolites, contained in groups i and iv, were identified. These findings provide new evidence in support of the hypothesis that brown rot fungi may be capable of producing hydroxyl radicals, which could be utilized to degrade wood and certain xenobiotics.

Fluoroquinolones (FQs) have found wide application in human and veterinary medicine. They are active against a broad spectrum of pathogenic gram-negative and gram-positive bacteria (18, 49). Enrofloxacin (Fig. 1) has been developed for veterinary use to treat infections in pet animals and livestock (7, 44). In mammals, FQs can be metabolized by glucuronidation, sulfation, N dealkylation, and oxidation of the amine substituent (27, 42). However, a major fraction is excreted unchanged and introduced into the environment via animal waste (51). Furthermore, manure from livestock is often disposed of by being spread onto agricultural soil and pastures.

Little is known about both the biodegradability and fate of antibiotics in the environment (17, 21, 31). Fluorinated aromatic compounds, as exemplified by FQs, are xenobiotics; i.e., they are man-made and have not been found to occur naturally (20, 36). However, FQs are tightly bound to soil and feces (13, 31, 34). In contrast to earlier views, such binding might be regarded as being quite a favorable characteristic of a substance (23), because bound molecules should hardly be bioavailable. As a consequence, FQs might not exert a significant selection pressure in situ, e.g., in eliminating specific parts of a bacterial population or in selecting for resistance. However, strong binding can be expected to delay degradation and may partly explain the apparent recalcitrance of FQs (21, 31).

Biodegradation of sarafloxacin, an FQ used in poultry medicine, has been studied in three different types of soils. From [2-^{14}C]sarafloxacin, $\leq$0.6% $^{14}CO_2$ was produced after 80 days (31). In another investigation, the persistence of sarafloxacin (among other antibiotics) in a marine sediment was assessed. Its apparent depuration was attributed to leaching and redistribution rather than to degradation (21).

Recently, we have shown in vitro degradation of enrofloxacin by the white rot fungus *Phanerochaete chrysosporium* and by *Gloeophyllum striatum*, representing the brown rot fungi. After 4 weeks of incubation, 6 and 16% $^{14}CO_2$, respectively, were produced from [4-^{14}C]enrofloxacin in liquid cultures (45). Furthermore, four species of white rot fungi and three strains of *G. striatum* were found to degrade [4-^{14}C]enrofloxacin bound to straw by up to 50% within 8 weeks. Enrofloxacin preadsorbed to agricultural soil could also be metabolized, although at a much lower rate, possibly reflecting decomposition of the matrix to which the drug was bound (33).

White rot fungi like *P. chrysosporium* are known to degrade the lignin component of woody plant cell walls as well as a wide spectrum of pollutants such as polyaromatic hydrocarbons, polychlorinated biphenyls, chlorinated pesticides (e.g., dichlorodiphenyltrichloroethane and lindane), and explosives (e.g., trinitrotoluene) (4, 6, 8–10, 15, 35). Such activities were attributed to lignin peroxidases, manganese-dependent peroxidases, and laccases. These extracellular enzymes are thought to catalyze oxidative degradation reactions via diffusible agents like aryloxy radicals, Mn^{3+}, and even hydroxyl radicals, with the latter being produced by secondary reactions. Mechanistically, none of these processes is fully understood (4, 14, 15, 19, 25).

Brown rot fungi preferentially degrade the cellulose and hemicellulose components of plant cell walls, while lignin has been shown to be modified primarily by hydroxylation and demethylation and to a minor extent by depolymerization (15, 32). For the decay of wood, a Fenton-type reaction mechanism was first postulated by Koenigs (30). In various model systems,

* Corresponding author. Phone: 49 2173 38 4882. Fax: 49 2173 38 3766.

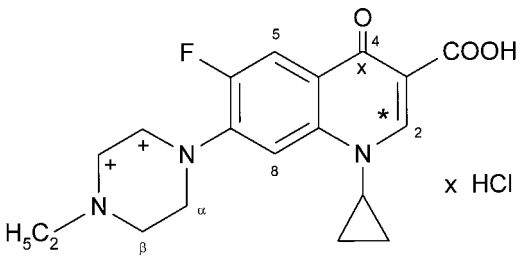

FIG. 1. Molecular structure of enrofloxacin and positions of the ^{14}C label in [2-^{14}C]enrofloxacin (*), [4-^{14}C]enrofloxacin (×), and [piperazine-2,3-^{14}C]enrofloxacin (+).

hydroxyl radicals are thought to be produced by a reductive cleavage of hydrogen peroxide by Fe^{2+} (15, 19, 25, 28, 50): $Fe^{2+} + H_2O_2 \rightarrow Fe^{3+} + HO^{\cdot} + HO^{-}$.

Iron is abundant in decaying wood, while hydrogen peroxide could be generated by enzymes like cellobiose dehydrogenase, aryl alcohol oxidase, or glyoxal oxidase. Superoxide radicals also have to be considered as a potential source of hydroxyl radicals (15, 19, 22, 24, 30, 37, 50). A partially purified glycopeptide from *Tyromyces palustris* was proposed to catalyze both the formation of hydrogen peroxide from superoxide radicals and the subsequent reduction of hydrogen peroxide by bound Fe^{2+} (22). Moreover, the formation of hydroxyl radicals during growth of *Antrodia xantha* on wood shavings has been demonstrated by a chemiluminescence method utilizing phthalic hydrazide as radical trap (3).

For our attempts to identify some of the metabolites formed during the degradation of enrofloxacin, we selected the brown rot fungus *G. striatum* DSM 9592. This strain did not exhibit any peroxidase or laccase activity typical of white rot fungi, despite having the highest activity in degrading enrofloxacin of all wood-rotting basidiomycetes studied so far (33, 45).

MATERIALS AND METHODS

Organism. *G. striatum* DSM 9592 degraded enrofloxacin in liquid culture (45) and bound to straw (33) but exhibited neither lignin peroxidase, laccase, nor tyrosinase activity when tested by the methods described by Stalpers (40); ABTS [2,2′-azinobis(3-ethylbenzthiazoline-6-sulfonic acid)], which is used for the detection of laccase (38), also was not oxidized (43).

Culture media and growth conditions. Stock cultures of *G. striatum* were kept on malt extract agar CM 59, pH 5.4 (Oxoid) (Unipath, Wesel, Germany), containing (per liter) 15 g of malt extract, 2.5 g of mycological peptone, and 15 g of agar. Cultures on agar plates were incubated at room temperature for at least 7 days. To inoculate liquid cultures, small agar pieces were cut out of the agar. Precultures in liquid medium were grown in malt extract broth CM 57, pH 5.5 (Oxoid). Five grams of dry substance was dissolved in 1 liter of deionized water and distributed in portions of 30 ml into 250-ml Erlenmeyer flasks. These were sealed with a cotton plug and autoclaved for 10 min at 115°C.

Mineral medium. The unbuffered mineral medium, devoid of a carbon, nitrogen, or phosphate source, contained 0.8 mM $MgSO_4$, 0.2 mM $CaCl_2$, 12 μM H_3BO_3, 0.4 μM $CoSO_4$, 0.2 μM $CuSO_4$, 0.04 μM $(NH_4)_6Mo_7O_{24}$ (Merck, Darmstadt, Germany), 2 μM $MnSO_4$, and 0.4 μM $ZnSO_4$ (Riedel-deHaën, Seelze, Germany). This medium was sterilized at 121°C for 20 min. Prior to inoculation, it was supplemented with 20 μM $FeSO_4$ (Riedel-deHaën) and 1 ml (per liter of medium) of a vitamin stock solution containing (per liter) 20 mg of 4-aminobenzoic acid sodium salt, 6 mg of D-(+)-biotin, 50 mg of DL-α-lipoic acid, 50 mg of nicotinamide, 10 mg of D-(+)-pantothenic acid sodium salt, 100 mg of pyridoxine · HCl, 50 mg of (−)-riboflavin (Aldrich, Steinheim, Germany), 20 mg of folic acid (Fluka, Neu-Ulm, Germany), 10 mg of thiamine · HCl (Merck), 20 mg of thiamine pyrophosphate chloride, and 50 mg of cyanocobalamin (Sigma, Deisenhofen, Germany). Sterile-filtered stock solution was stored frozen until use. The final pH of around 6 was maintained throughout the incubation period.

Enrofloxacin and reference compounds. The chemical structure of enrofloxacin · HCl [1-cyclopropyl-7-(4-ethyl-1-piperazinyl)-6-fluoro-1,4-dihydro-4-oxo-3-quinolinecarboxylic acid hydrochloride], including the positions of ^{14}C labeling, is shown in Fig. 1. The unlabeled standard compound was provided by H. Rast (Bayer AG, Leverkusen, Germany); its chemical purity was >99.4%. Chemically synthesized reference compounds (Table 1) were kindly provided by W. Hallenbach (Bayer AG) (F-6, F-8, and F-11) and U. Petersen (Bayer AG) (F-4 and F-9).

Radioactively labeled enrofloxacin. ^{14}C-labeled enrofloxacin was synthesized by R. Koch (Bayer Corp., Stilwell, Kans.) (C-2 and C-4 label) and by R. Thomas and R. Körmeling (Bayer AG, Wuppertal, Germany) (piperazine label). In the latter laboratory, all labeled substrates were freshly purified immediately before use. The specific activities of [4-^{14}C]-, [2-^{14}C]-, and [piperazine-2,3-^{14}C]enrofloxacin · HCl were 4.98, 0.63, and 3.38 MBq/mg, respectively; the radiochemical purity was >98%, as determined by high-performance liquid chromatography (HPLC). The compounds were dissolved in sterile distilled water and stored frozen until use.

Experimental procedures. Precultures of *G. striatum* were grown in malt broth, unagitated, at room temperature for 7 days. After the supernatant was discarded, each mycelium (22 ± 4 mg [dry weight] [mean ± standard deviation for quadruplicate assays]) was washed once with 30 ml of mineral medium (with vitamins omitted) before being transferred to the culture vessels of test system A or B. Dry weight was determined on cellulose acetate membrane filters (pore size, 0.45 μm; Sartorius, Göttingen, Germany) which had been dried to a constant weight at 85°C overnight.

Test system A was employed to determine the degradation kinetics of [^{14}C]enrofloxacin. The reaction vessel is described elsewhere (1). Briefly, each 100-ml screw-capped jar contained 10 ml of sterile mineral medium and a sterile 10-ml glass tube holding 3 ml of 1 M NaOH as a trap for CO_2. To prevent volatile ^{14}C-labeled metabolites from entering the NaOH, a bore hole in the tube wall was loosely sealed with a cotton plug coated with 2% (wt/vol) paraffin in hexane. Each flask received 2.2 ± 0.4 mg (dry weight) of mycelium per ml. ^{14}C-labeled enrofloxacin (8 to 9 kBq) was diluted with unlabeled drug to give a final concentration of 10 ppm. All experiments were run at room temperature in the dark to prevent photodegradation of enrofloxacin.

Test system B was utilized for the production of metabolites. Each 250-ml Erlenmeyer flask, containing 30 ml of mineral medium, was inoculated with 2.2 ± 0.4 mg (dry weight) of mycelium per ml. Thereafter, 300 μg of enrofloxacin, ^{14}C labeled with 448.5, 229.1, or 691.9 kBq (of C-4, C-2, or piperazine label, respectively), was added. The vessels were kept at 150 rpm at room temperature in the dark. Produced CO_2 was adsorbed to 6 g of soda lime placed in a funnel at the top of the flask. To determine produced $^{14}CO_2$, the soda lime was acidified with 5 M HCl. Released $^{14}CO_2$ was transferred into scintillation fluid via a stream of nitrogen (see below).

In order to produce the quantity of a metabolite required for structure elucidation by ^1H nuclear magnetic resonance (NMR) (approximately 20 μg), 180 ml of supernatant from 2-day-old cultures containing degraded [4-^{14}C]enrofloxacin

TABLE 1. Nomenclature of metabolites generated by *G. striatum* from enrofloxacin

Designation	Chemical name
F-1	1-Cyclopropyl-7-(4-ethyl-1-piperazinyl)-6-fluoro-3-hydroxy-4-*1H*-quinolinone
F-2	1-Cyclopropyl-7-(4-ethyl-1-piperazinyl)-1,4-dihydro-6-hydroxy-4-oxo-3-quinolinecarboxylic acid
F-3	1-Cyclopropyl-6-(4-ethyl-1-piperazinyl)-5-fluoro-*1H*-indole-2,3-dione
F-4[a]	1-Cyclopropyl-7-{[2-(ethylamino)ethyl]amino}-6-fluoro-1,4-dihydro-4-oxo-3-quinolinecarboxylic acid
F-5	1-Cyclopropyl-7-(4-ethyl-1-piperazinyl)-1,4-dihydro-6,8(5,6)-dihydroxy-4-oxo-3-quinolinecarboxylic acid
F-6[a]	1-Cyclopropyl-7-(4-ethyl-1-piperazinyl)-6-fluoro-1,4-dihydro-8-hydroxy-4-oxo-3-quinolinecarboxylic acid
F-7	1-Cyclopropyl-7-(4-ethyl-1-piperazinyl)-6-fluoro-1,4-dihydro-5,8-dihydroxy-4-oxo-3-quinolinecarboxylic acid
F-8[a]	1-Cyclopropyl-6-fluoro-1,4-dihydro-7,8-dihydroxy-4-oxo-3-quinolinecarboxylic acid
F-9[a]	7-Amino-1-cyclopropyl-6-fluoro-1,4-dihydro-4-oxo-3-quinolinecarboxylic acid
F-10[a]	1-Ethylpiperazine
F-11[a]	2-Cyclopropylamino-4-(4-ethyl-1-piperazinyl)-5-fluorobenzoic acid

[a] A chemically prepared reference compound is available.

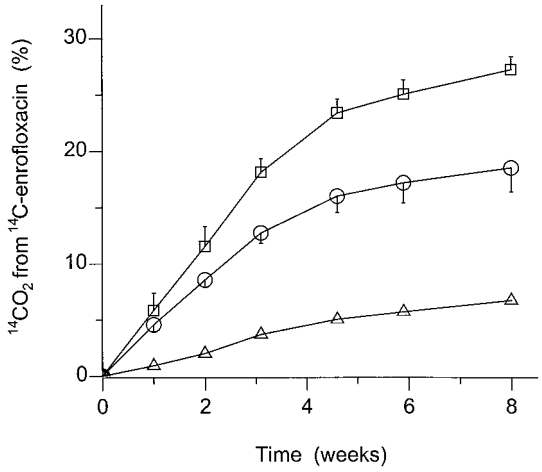

FIG. 2. Total $^{14}CO_2$ production from [^{14}C]enrofloxacin by *G. striatum*. Mycelia, pregrown in malt medium, were washed and transferred into a defined mineral medium containing 10 ppm of enrofloxacin labeled either at C-2 (□), at C-4 (○), or in the piperazinyl moiety (△). Values given are the means ± standard deviations for five replicate cultures.

was produced. Each of six replicate cultures was first checked by HPLC to verify the expected metabolite pattern. After separation of the mycelia by centrifugation, combined supernatants were lyophilized, redissolved in 8.5 ml of distilled water, analyzed, and fractionated by HPLC method I (see below).

HPLC. Analytical and micropreparative HPLCs were performed on an HPLC system HP 1050 equipped with a diode array detector (Hewlett-Packard, Waldbronn, Germany), a Ramona 90 radioactivity flowthrough detector (Raytest, Straubenhardt, Germany), and a Kromasil 100 C_{18} column (0.46 by 25 cm; particle size, 5 μm; Eka-Chemicals, Bohuds, Sweden). The elution solvent consisted of 0.1 mM ammonium formate in 1% formic acid (component A) and acetonitrile (component B). Routinely, the following gradient was employed (HPLC method I): starting at 100% component A for 2 min, component A was linearly decreased to 94% over 3 min and then to 85% over 10 min. Thereafter, component A was kept at 85% for 15 min and then decreased to 72% over 5 min and finally to 0% over 10 min. For micropreparative purification of isolated metabolites, HPLC method II was used, in which component A contained, in addition, 1% (vol/vol) isopropanol. The flow rate was 1 ml/min.

HPLC-MS. Combined HPLC-electrospray ionization mass spectrometry (HPLC-MS) was performed on an HPLC system HP 1090 (Hewlett-Packard) equipped with a Kromasil 100 C_{18} column (0.2 by 25 cm; particle size, 5 μm; Eka-Chemicals), linked to a TSQ 7000 mass spectrometer (Finnigan-MAT, Bremen, Germany), which was operated in the electrospray ionization mode. The atmospheric pressure ionization source (Finnigan) was controlled by a DECstation computer system (Digital Equipment Corp., Maynard, Mass.). Applied gradients were as described above. The effluent of the HPLC column (200 μl/min) was passed on to the MS interface without splitting. The spray needle voltage was 4.5 kV, and nitrogen at 500 kPa served as the sheath gas. The capillary was held at 210°C. The electrospray ionization ion source was used in the positive mode, scanning the range of *m/z* 150 to 900 in 2.5 s. For the identification of F-10 (see below), a scan range of *m/z* 30 to 600 was used.

^{1}H-NMR spectroscopy. NMR spectra were recorded at 500 MHz on a Bruker NMR spectrometer AMX 500 (Bruker, Rheinstetten, Germany) in D_2O (deuteration degree, ≥99.96%) containing 0.1 or 5% (vol/vol) trifluoroacetic acid-d_1. Chemical shifts are reported in parts per million (δ). Acetone was used as an internal standard (δ = 2.00 ppm).

Liquid scintillation counting. An LS 3801 liquid scintillation counter (Beckman, Fullerton, Calif.) was employed for determination of radioactivity at ambient temperature. Radioactivities in stock solutions and small-volume samples were determined in Instant-Scint-Gel Plus (Beckman). The sodium hydroxide solution of test system A was transferred into 7 ml of Quickszint 401 (Zinser Analytic, Frankfurt, Germany). Remobilized CO_2 was trapped in a mixture of 5.6 ml of Permafluor V and 4.4 ml of Carbosorb (Beckman).

Fenton's reaction. The reaction mixture described previously (28) was modified and consisted of 10 ml of 1 mM sodium acetate buffer (pH 4.2) containing 5 μM $FeSO_4$, 0.01% hydrogen peroxide, and 10 ppm of [4-^{14}C]enrofloxacin (141 kBq). After 4 h of incubation at room temperature in the dark with stirring at 100 rpm, the solution was frozen and lyophilized. The resulting dry matter was redissolved in 0.5 ml of distilled water and analyzed by HPLC and HPLC-MS as described above. Metabolites formed from enrofloxacin were characterized by retention time, molecular weight, and the characteristic isotope pattern caused by the ^{14}C label.

RESULTS

Kinetics of $^{14}CO_2$ formation from [^{14}C]enrofloxacin. Precultured mycelia were resuspended in a defined mineral medium containing 10 ppm of enrofloxacin, which was ^{14}C labeled at either of three different positions (Fig. 1). After 8 weeks, 27.3% ± 1.1% and 18.5% ± 2.1% $^{14}CO_2$ were produced from [2-^{14}C]- and [4-^{14}C]enrofloxacin, respectively. Under identical conditions, only 6.7% ± 0.4% $^{14}CO_2$ was generated from [piperazine-2,3-^{14}C]enrofloxacin (Fig. 2). The maximum rate of CO_2 formation (observed with [2-^{14}C]enrofloxacin) was 5.8% ± 1.5% per week, which corresponds to a specific activity of 2.6 ± 0.7 nmol of CO_2 per mg (dry weight) of mycelium per week. Nonspecific binding of ^{14}C-labeled compounds to mycelium was assessed by a series of balances of radioactivity employing cultures of ages varying from 2 to 42 days. Recoveries were close to 100% throughout. For example, in 5-day-old cultures containing [4-^{14}C]enrofloxacin, the amounts of (i) produced $^{14}CO_2$, (ii) activity remaining in the supernatant, and (iii) activity nonspecifically bound to mycelium had reached 4.3% ± 1.7%, 90.6% ± 2.3%, and 4.2% ± 0.4% (mean ± standard deviations for three cultures), respectively (data not shown in detail).

The determination of the incubation time resulting in maximum concentrations of major metabolites is shown in Fig. 3. After 5 days, enrofloxacin had a residual concentration of only 9%, and it was hardly detectable from day 7 onwards (not shown). The HPLC elution profiles indicated five major metabolites, reaching similar maximum concentrations after 2 days. Hence, an incubation time of 2 days was used to produce metabolites for structure elucidation.

Profiles of metabolites generated from enrofloxacin. Cultures of *G. striatum*, each containing either [2-^{14}C]-, [4-^{14}C]- or [piperazine-2,3-^{14}C]enrofloxacin, were incubated under identical conditions for 2 days. Supernatants were analyzed by HPLC with radioactivity detection. Representative elution profiles are shown in Fig. 4. All major metabolites, arbitrarily designated F-1, F-2, and F-4 to F-7 (F indicates their fungal origin), were present in all three supernatants, regardless of the applied label. Obviously, C-2, C-4, and the piperazinyl

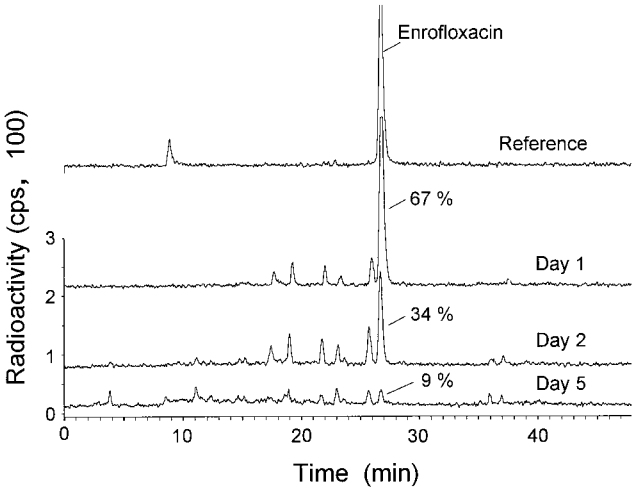

FIG. 3. Degradation of [4-^{14}C]enrofloxacin and time course of formation of major metabolites by *G. striatum*. Mycelia were transferred into mineral medium containing 10 ppm of enrofloxacin. The supernatant was analyzed by HPLC to determine the pattern of metabolites formed after up to 5 days. Due to the use of a different HPLC column, the retention times here were slightly smaller than those indicated in Table 2.

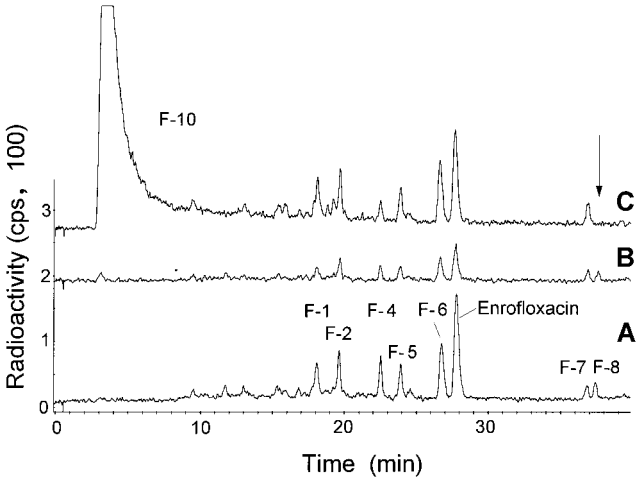

FIG. 4. HPLC analysis of 2-day-old supernatants from cultures of *G. striatum* containing metabolites generated from [^{14}C]enrofloxacin. Enrofloxacin had a concentration of 10 ppm and was labeled at one of three alternative positions: either [4-^{14}C]enrofloxacin (A), [2-^{14}C]enrofloxacin (B), or [piperazine-2,3-^{14}C] enrofloxacin (C) was used. In trace C, the apparent loss of F-8 is marked by an arrow; also note the oversized peak of F-10.

moiety all had been retained. The maximum concentrations of such metabolites fell between 6% (F-5) and 13% (F-6) of the initially applied radioactivity. Metabolite F-8 was missing in the profile generated from piperazine-labeled enrofloxacin (Fig. 4, trace C). In addition, a broad and tailing, oversized peak appeared in the front of that chromatogram. This fraction comprised a polar compound, designated F-10, which was gradually retained by the solid-state scintillator of the detector cell, thereby causing such an artificially enlarged signal. When this fraction was collected and analyzed with an LS counter, an appropriate amount of radioactivity (approximately 13%) was found.

F-10. HPLC-MS analysis of supernatant containing degraded [piperazine-2,3-^{14}C]enrofloxacin directly permitted the identification of F-10 (1-ethylpiperazine) by its pseudomolecular ion $(M + H)^+$ at *m/z* 115 and by its specific ion pattern (*m/z* 115/117/119 = 10:1:2), caused by the presence of either one or two ^{14}C-labeled carbon atoms in the piperazinyl moiety (Table 2). A corresponding pattern found in [piperazine-2,3-^{14}C]enrofloxacin at *m/z* 360, 362, and 364 proved that F-10 was a specific derivative thereof.

Identification of metabolites by HPLC cochromatography. Supernatant containing degraded [4-^{14}C]enrofloxacin was analyzed by HPLC cochromatography with UV detection. Four metabolites (F-4, F-6, F-8, and F-9) could be identified by coelution with chemically prepared reference compounds. The systematic names of all identified metabolites are listed in Table 1; the corresponding chemical structures are shown in Fig. 5. HPLC retention times of all metabolites, their pseudomolecular ions, and characteristics of their UV absorption spectrum are given in Table 2. The UV spectra of F-4, F-6, F-8, and F-9 were identical to those of the respective reference compounds.

Structure elucidation by ^{1}H-NMR spectroscopy. Fractions containing major metabolites were isolated from the combined supernatant preparation and subjected to HPLC-MS and, finally, NMR analysis.

(i) F-1. After separation of a nonradioactive matrix component, the fraction containing F-1 (Table 1) was subjected to HPLC-MS. Its mass of 331 Da indicated a loss of 28 mass units (Table 2). The NMR spectrum of F-1, shown in Fig. 6, was very similar to that of enrofloxacin (Table 3). All proton signals of the cyclopropyl and the ethylpiperazinyl moieties could be assigned. The aromatic protons H-5 and H-8 had almost identical chemical shifts (δ) as well as H,F coupling constants ($J_{H,F}$). However, the signal of H-2 was shifted upfield (δ = 8.37 ppm instead of 8.65 ppm), indicating the replacement of the carboxyl group by the electron-rich hydroxyl group, which was in agreement with the determined molecular weight. The proposed structure of F-1 is shown in Fig. 5.

(ii) F-2. The molecular weight of metabolite F-2 (Table 1) was 357 (Table 2). Its NMR spectrum showed only one—but a decisive—difference when compared with enrofloxacin: the signals of H-5 and H-8 did not exhibit H,F coupling, indicating the loss of the fluorine atom (Table 3). The molecular mass of F-2, two mass units smaller than enrofloxacin, was in agreement with a hydroxyl group replacing fluorine (Fig. 5).

(iii) F-4. Metabolite F-4 (Table 1), identified primarily by retention time and UV absorption spectrum, had a molecular weight of 333 (Table 2). Even after further purification, the NMR spectrum indicated the presence of matrix components superimposed on the aliphatic region. The aromatic region, however, provided the signals of protons H-2, H-5, and H-8; these were identical in chemical shift and multiplicity to the signals of the reference compound (data not shown). Further attempts to purify F-4 failed, because of its lability.

TABLE 2. HPLC retention times, pseudomolecular ions in MS, and characteristics of the UV absorption spectra of [4-^{14}C]enrofloxacin and metabolites

Characteristic	Value for:											
	Enrofloxacin	F-1	F-2	F-3	F-4	F-5	F-6	F-7	F-8	F-9	F-10[c]	F-11
Retention time[a] (min)	27.7	18.1	19.5	—[b]	22.4	24.6	26.7	36.7	37.2	38.5	2.5	28.4[e]
Pseudomolecular ion[d] $(M + H)^+$ (*m/z*)	360	332	358	318	334	374	376	392	280	263	115	308
UV absorption (nm)												
λ_{max} (major)	278	283	278	—[b]	276	288	245	247	272	271		250[e]
λ_{max} (minor)	316, 328		346		339	260	330	353	250, 327			278[e], 352[e]
Shoulder			335			338	271	264				

[a] Determined by HPLC method I, as described in Materials and Methods.
[b] —, not detectable by HPLC with either UV or radioactivity detection.
[c] Data are derived from an experiment with [piperazine-2,3-^{14}C]enrofloxacin.
[d] $(M + H)^+$ was accompanied by $(M + 2 + H)^+$ resulting from the ^{14}C label; in addition, $(M + 4 + H)^+$ was present in F-10.
[e] Generated from the reference substance.

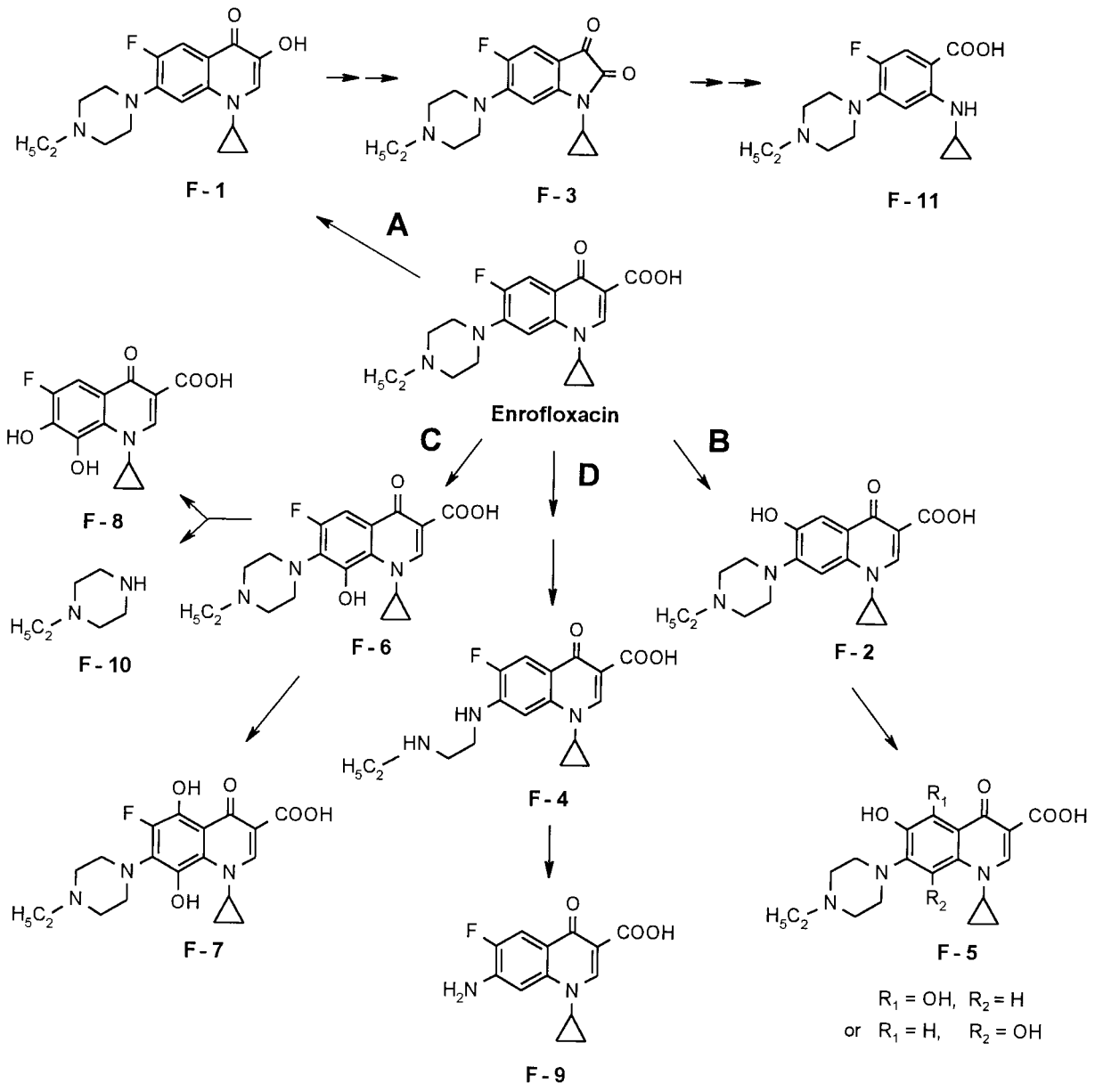

FIG. 5. Proposed principle routes of degradation of enrofloxacin (routes A to D) employed by the brown rot fungus *G. striatum*. Monohydroxylated metabolites (F-1, F-2, and F-3) may result from an initial attack of enrofloxacin by hydroxyl radicals at different sites of the molecule. Secondary and subsequent attacks at one of various possible sites in each of these primary metabolites may cause branching of the routes, resulting in a network of metabolites. However, only the most stable intermediates could be isolated and characterized.

(iv) F-5. Metabolite F-5 (Table 1) had a molecular weight of 373 (Table 2). This could have resulted from an elimination of fluorine, combined with a twofold hydroxylation. Due to matrix components, the aliphatic region of its NMR spectrum could not be analyzed. However, in the aromatic region two signals were detected. A singlet at 8.58 ppm could be specifically assigned to H-2. Another singlet at 7.02 ppm (absence of H,F coupling) indicated the loss of fluorine. Because of the absence of a further aromatic proton signal, and based on the molecular weight, two structural alternatives have to be envisaged: a 5,6- or a 6,8-dihydroxylated congener of enrofloxacin (Fig. 5). F-5 was rapidly decomposed.

(v) F-6. Identified primarily by cochromatography, metabolite F-6 (Table 1) had a molecular weight of 375 (Table 2). After purification, i.e., separation from enrofloxacin, F-6 was analyzed by NMR. The spectrum contained all signals typical of the ethylpiperazinyl and the cyclopropyl groups (Table 3). Only two protons were detected in the aromatic region, a singlet assigned to H-2 and a doublet specifically assigned to H-5 due to *ortho* coupling with fluorine (Table 3). Since the molecular mass was increased by 16 Da, F-6 was identified as 8-hydroxyenrofloxacin (Fig. 5). The reference compound showed an identical NMR spectrum (not shown).

(vi) F-7. The molecular weight of 391 determined for F-7 suggested a twofold hydroxylation (Tables 1 and 2). The NMR spectrum of F-7 revealed only one singlet at 8.77 ppm, typical of H-2. Hence, the two hydroxyl groups could have been introduced only at C-5 and C-8 (Fig. 5). Matrix compounds

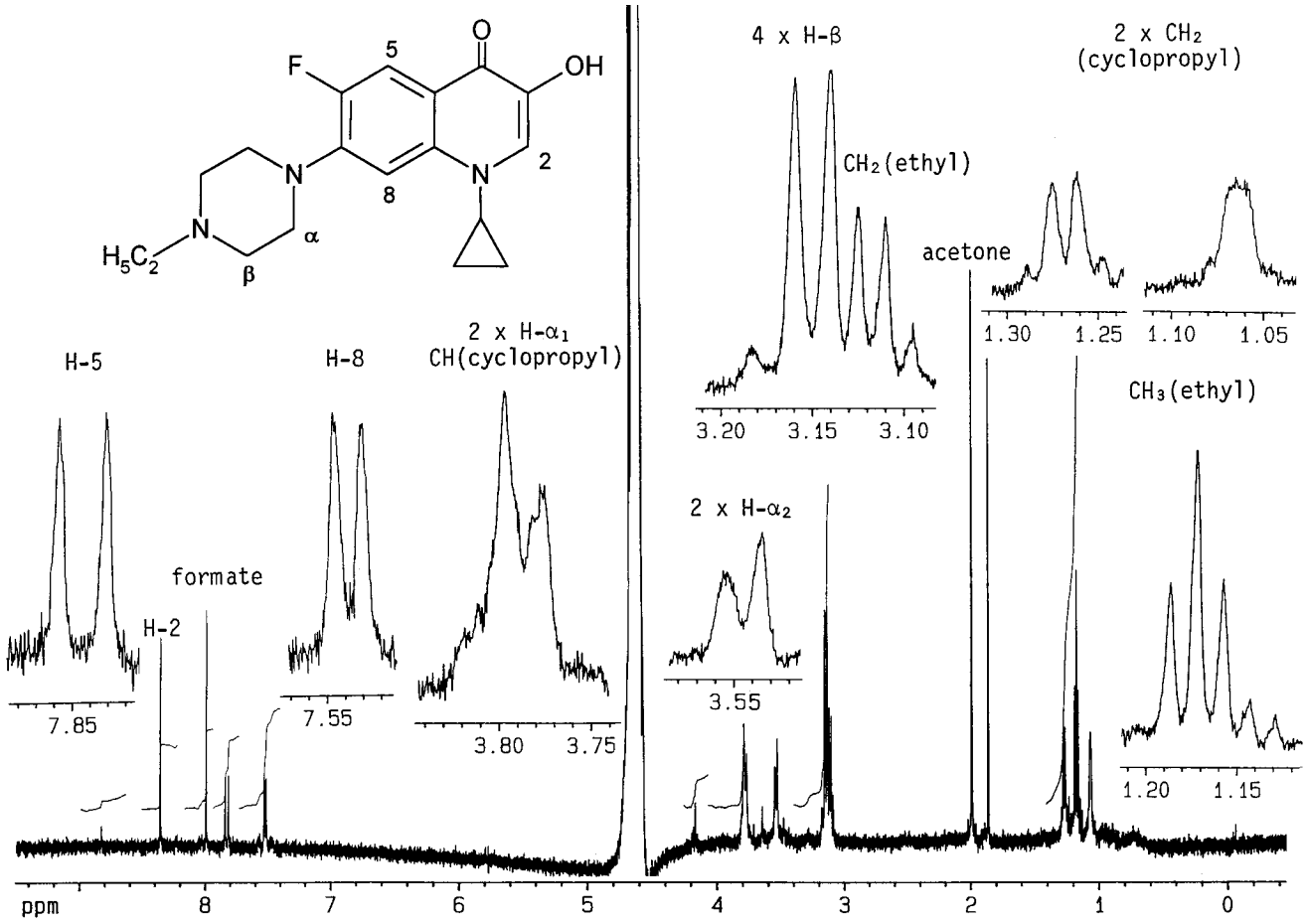

FIG. 6. The 500-MHz ^{1}H-NMR spectrum (including expanded areas) of the decarboxylated congener of enrofloxacin (F-1) formed by *G. striatum.*

masked the aliphatic region and prevented further NMR assignments. F-7 was already decomposed during purification.

(vii) F-8. Metabolite F-8 (Table 1) was first identified by cochromatography. Its molecular weight of 279 (Table 2) was indicated by ions at *m/z* 280 and 262 [$(M + H)^+$ and $(M + H - H_2O)^+$], which were also observed with reference compound. The NMR spectrum showed that the 1-ethylpiperazine moiety had been cleaved off (compare with Fig. 4, trace C). Only two aromatic protons were present, H-5 (d, δ = 7.57 ppm, $J_{H,F}$ = 10.1 Hz) and H-2 (s, δ = 8.82 ppm). Two 2H multiplets (at 0.99 and 1.10 ppm) and a 1H multiplet (at 4.18 ppm) were charac-

TABLE 3. ^{1}H-NMR data for enrofloxacin and monohydroxylated metabolites[a]

Proton(s)[b]	Enrofloxacin				F-1				F-2				F-6			
	δ (ppm)	Integral	Multiplicity	*J* (Hz)	δ (ppm)	Integral	Multiplicity	*J* (Hz)	δ (ppm)	Integral	Multiplicity	*J* (Hz)	δ (ppm)	Integral	Multiplicity	*J* (Hz)
CH_2 (cyclopropyl)	1.01	2	m		1.06	2	m		1.07	2	m		0.98	2	m	
CH_3 (ethyl)	1.17	3	t	7.3	1.17	3	t	7.3	1.18	3	t	7.3	1.17	3	t	7.4
CH_2 (cyclopropyl)	1.21	2	m		1.27	2	m		1.26	2	m		1.08	2	m	
CH_2 (ethyl)	3.12	2	q	7.3	3.12	2	q	7.3	3.12	2	q	7.3	3.11	2	q	7.4
CH_2 (piperazine, H-β)	3.15	4	m		3.15	4	m		3.10	4	m		≈3.2	4	m	
CH_2 (piperazine, H-α_2)	3.54	2	m		3.54	2	m		3.55	2	m		3.42	2	m	
CH (cyclopropyl)	3.58	1	m		≈3.8	1	m		3.74	1	m		4.20	1	m	
CH_2 (piperazine, H-α_1)	3.79	2	m		3.79	2	m		3.90	2	m		3.49	2	m	
H-8	7.45	1	d	7.2[c]	7.54	1	d	7.5[c]	7.54	1	s					
H-5	7.66	1	d	13.0[c]	7.85	1	d	12.8[c]	7.52	1	s		7.41	1	d	11.5[c]
H-2	8.65	1	s		8.37	1	s		8.84	1	s		8.76	1	s	

[a] Spectra were determined at 500 MHz in a deuterated solvent (0.1% trifluoroacetic acid-d_1 in D_2O for enrofloxacin and 5% trifluoroacetic acid-d_1 in D_2O for F-1, F-2, and F-6). Acetone was used as internal standard (δ = 2.00 ppm). Multiplicities are abbreviated as follows: s, singlet; d, doublet; t, triplet; q, quadruplet; m, multiplet.

[b] Positioning is as shown in Fig. 1.

[c] $J_{H,F}$.

teristic of the cyclopropyl moiety. The structure of F-8 is shown in Fig. 5.

Identification of minor metabolites by HPLC-MS. HPLC-MS analysis revealed three additional minor metabolites, which could not be unequivocally assigned in HPLC elution profiles by either UV or radioactivity detection because of their very low concentrations.

(i) F-3. Metabolite F-3 (Table 1), with a molecular weight of 317 (Table 2), showed in mass spectra the characteristic ion patterns generated from supernatants containing [4-^{14}C]enrofloxacin (*m/z* 318 and 320) or [piperazine-2,3-^{14}C]enrofloxacin (*m/z* 318, 320, and 322). The specific signal at *m/z* 320 was absent when [2-^{14}C]enrofloxacin was employed as a substrate, indicating that C-2 of enrofloxacin was eliminated in F-3. Based on these observations, an isatin-type structure was proposed for F-3 (Fig. 5).

(ii) F-9. Metabolite F-9 (Table 1), initially identified by cochromatography, had a molecular weight of 262 (Table 2). In order to further confirm its structure, the supernatant was spiked by adding approximately the same concentration of unlabeled reference compound. Analysis by HPLC-MS revealed the expected isotope dilution effect: the height of the signal at *m/z* 265 (caused by [4-^{14}C]enrofloxacin) was reduced to about 50%. The proposed structure of F-9 is given in Fig. 5.

(iii) F-11. The identification of metabolite F-11 (Table 1; Fig. 5) had to be based on an analysis of the reference compound, which had a molecular weight of 307 (Table 2); it proved to be quite labile in aqueous solution. When HPLC-MS was done in the single-ion monitoring mode at *m/z* 308, a peak was detected in the supernatant at the retention time of the reference compound (Table 2). To further assess its specificity, a supernatant sample was spiked with reference compound. As expected, an enlarged peak was observed in the single-ion trace at *m/z* 308, indicating the presence of F-11 in the supernatant of *G. striatum.*

Metabolites at trace concentrations. Approximately 10 additional metabolites of enrofloxacin were detected by HPLC-MS. Most had retained all ^{14}C labels (C-2, C-4, and piperazine) and showed the specific patterns of pseudomolecular ions. Five examples of such molecular weights and hypothetical structures should be mentioned (compare with Fig. 5): a molecular weight of 305 would be in agreement with an oxidatively decarboxylated F-4, a mass of 329 Da could result from oxidatively decarboxylated F-2, a 347-molecular-weight metabolite may have been derived from F-1 by hydroxylation at C-8 or C-5, a 349-molecular-weight metabolite could have been generated from F-4 hydroxylated at C-8 or C-5, and a metabolite with a molecular weight of 389 might have been generated from metabolite F-2 by twofold hydroxylation at C-5 and C-8 or, alternatively, by oxidation of F-7, giving rise to the respective quinone. In fact, two metabolites with a molecular weight of 389 were observed at distinct retention times. However, due to the extremely low concentrations of these metabolites, which probably reflect their lability, no additional information could be obtained.

Fenton's reaction. [4-^{14}C]enrofloxacin was degraded by Fenton's reaction as described in Materials and Methods. A typical HPLC elution profile is shown in Fig. 7. Five metabolites were identified by HPLC-MS, namely, three monohydroxylated congeners of enrofloxacin (F-1, F-2, and F-6) and two metabolites (F-4 and F-9) indicating degradation of the piperazinyl substituent. The systematic names and analytical characteristics of identified metabolites are given in Tables 1 and 2.

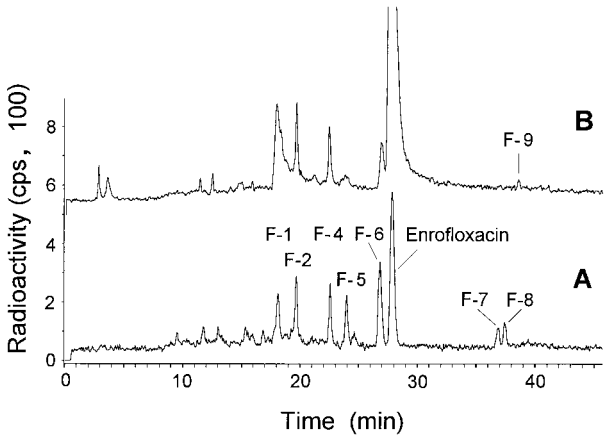

FIG. 7. Comparison of HPLC elution profiles showing metabolites generated by *G. striatum* from [4-^{14}C]enrofloxacin (A) and metabolites produced by chemical degradation of [4-^{14}C]enrofloxacin with Fenton's reagent (B). The metabolites in trace B were identified by retention time, molecular weight, and ion pattern in MS.

DISCUSSION

In a previous paper, we described biodegradation of enrofloxacin adsorbed to straw. Three strains of the brown rot fungus *G. striatum* were found to possess a higher activity than four species of white rot fungi, including *P. chrysosporium* (33). Hence, we selected *G. striatum* for our attempts to identify the metabolites generated in this process. Because *G. striatum* did not exhibit peroxidase or laccase activity, which is typically found in white rot fungi (43), another degradation mechanism could be expected to be operative, possibly one of the Fenton type as first proposed by Koenigs for the decay of wood by brown rot basidiomycetes (30). Experimental conditions under which the lignocellulose-depolymerizing activity of a brown rot fungus could be induced in liquid culture have not been described before to our knowledge (29). However, we had initially observed that after the formation of biomass in malt broth, mycelia of *G. striatum* could be transferred into a defined mineral medium, lacking a carbon, nitrogen, and phosphorus source, to enhance the expression of the degradation potential for enrofloxacin, which otherwise remained undetectable, even in diluted malt medium (43).

Elimination kinetics of specific C atoms of enrofloxacin. At first, the degradation process was characterized by the formation of $^{14}CO_2$ from [^{14}C]enrofloxacin labeled either at position C-2, at position C-4, or in the piperazine ring. Because both the rate and extent of $^{14}CO_2$ production from [2-^{14}C]enrofloxacin were higher than those of $^{14}CO_2$ production from [4-^{14}C]enrofloxacin (Fig. 2), C-2 was most likely eliminated prior to C-4, which would be in accordance with degradation route A shown in Fig. 5. The high initial rates of $^{14}CO_2$ formation could not be maintained for incubation times exceeding 3 weeks. This was due either to the lack of nutrients or to unknown factors limiting *G. striatum* in this closed in vitro test system. It is remarkable that from [piperazine-2,3-^{14}C]enrofloxacin only about one-quarter of the amount of $^{14}CO_2$ was produced under identical conditions. Obviously, the core part of the quinolone molecule was the preferred target of the degradation activity expressed by *G. striatum*. As only about 5% of the ^{14}C label was nonspecifically bound to mycelium, the bulk of radioactivity, i.e., that in enrofloxacin and its metabolites, remained fully bioavailable in the supernatant.

Metabolites generated from enrofloxacin. HPLC elution profiles of supernatants from up-to-5-day-old cultures of *G. striatum* indicated that even the most abundant metabolites appeared only transiently. Already 2 days after the transfer from malt into mineral medium, the five major metabolites were reaching maximum concentrations (Fig. 3). When all three differently labeled enrofloxacin molecules were simultaneously employed in parallel cultures, almost identical patterns of metabolites were obtained (Fig. 4). Such profiles were composed of up to 25 peaks, as detected by HPLC-MS. Individual fractions were purified and analyzed by combining HPLC, HPLC-MS, and ^{1}H-NMR spectroscopy. The proposed molecular structures of 3 of 11 metabolites, F-1, F-2, and F-6 (chemical names are given in Table 1), could be confirmed by complete ^{1}H-NMR spectra. Four structures (those of F-4, F-5, F-7, and F-8) were ascertained by an analysis of the aromatic regions of their NMR spectra, while metabolites F-4, F-8, and F-9 could also be identified by cochromatography with chemically prepared reference compounds and by their UV absorption spectra. The identification of metabolites F-3, F-10, and F-11 had to be based on MS techniques.

The identified metabolites were assigned to four groups of compounds: (i) monohydroxylated congeners of enrofloxacin (F-1, F-2, and F-6), (ii) dihydroxylated congeners of enrofloxacin (F-5, F-7, and F-8), (iii) an isatin-type (F-3) and an anthranilic acid (F-11) derivative of enrofloxacin, and (iv) desethylene-enrofloxacin (F-4), the 7-amino congener of enrofloxacin (F-9), and 1-ethylpiperazine (F-10).

These groups of metabolites led us to propose the metabolic scheme shown in Fig. 5. It consists of four principle degradation routes, which, due to the similar concentrations of all major metabolites, might be simultaneously employed. Route A would be initiated by an oxidative decarboxylation. This irreversibly inactivates the drug, because the carboxyl group is essential for antibacterial activity of FQs (12). An isatin-type intermediate (F-3) as well as the anthranilic acid derivative (F-11) indicate cleavage of the heterocyclic core of enrofloxacin as well as the successive loss of C-2 and C-3, while C-4 was retained. Isatin is a known intermediate in degradation pathways of indole and tryptophan (2, 39). Liberation of $^{14}CO_2$ from [4-^{14}C]enrofloxacin (as shown in Fig. 2) involves F-11 and probably metabolites from the other degradation routes as well. The degradation of anthranilic acid is a well-documented natural process (2, 39).

Route B would be initiated by defluorination of enrofloxacin. This eliminates the xenobiotic structural element and reduces the antibacterial potential of metabolite F-2 (in terms of increased MICs) to $\leq$3% (12, 43). Route C could be initiated by hydroxylation of enrofloxacin at position C-8. This modification reduces the antibacterial potential of F-6 to $\leq$5% (43) and most likely enhances its further degradation. Dihydroxylated congeners are included in routes B and C. Such autoxidizable structures are prone to undergo further oxidative degradation, which might even include the cleavage of the homoaromatic part of enrofloxacin. Metabolites F-5, F-7, and F-8 were found to be decomposed already during purification, even in the frozen state.

Route D shows an oxidative degradation of the piperazinyl moiety. This sequence of reactions is apparently initiated by the formation of a carbonyl group, as was shown for ciprofloxacin (27). Degradation of F-4 should result in the formation of F-9, the 7-amino congener of enrofloxacin, which has a residual antibacterial activity on the order of $\leq$3%, as compared to the parent drug (43).

Proposed degradation mechanism. So far, the molecular mechanism of enrofloxacin degradation by *G. striatum* has not been studied in detail. However, degradation of enrofloxacin was very sensitive to hydroxyl-radical-scavenging agents like ethanol and dimethyl sulfoxide (19, 43). Hence, our results may represent new evidence in support of the hypothesis that brown rot fungi are able to catalyze the formation of hydroxyl radicals in a Fenton-type reaction. Under our experimental conditions, this mechanism might have been employed to degrade enrofloxacin. The proposed degradation routes, shown in Fig. 5, may reflect different sites of initial attack of enrofloxacin by hydroxyl radicals. Each of the primary metabolites offers various sites for a secondary attack, which would cause branching of the routes, resulting in the formation of a network of metabolites; this could explain the high number of metabolites observed by HPLC-MS. The molecular weights of some unidentified metabolites, detectable only by HPLC-MS, would be consistent with such a network.

Enrofloxacin was also chemically degraded by Fenton's reaction, in which hydroxyl radicals are generated from hydrogen peroxide and Fe^{2+} (50). The identification of all three characteristic monohydroxylated congeners of enrofloxacin as well as of the two typical intermediates indicating the degradation of the piperazinyl moiety supports the proposed role of hydroxyl radicals in *G. striatum*. The metabolic scheme outlined in Fig. 5 would be in agreement with the pattern of metabolites generated by Fenton's reaction, although it was not possible to isolate dihydroxylated metabolites from such reaction mixtures.

Preliminary experiments in our laboratory have shown that *G. striatum* gives rise to a pronounced chemiluminescence signal under the assay conditions described by Backa and colleagues (3), which has been proposed to directly indicate the formation of hydroxyl radicals in wood shavings. Degradation of lignocellulose and pollutants by reactions involving free radicals occurs extracellularly (4, 15, 25). However, the site of enrofloxacin degradation in *G. striatum* is not known at present.

In addition to the reactions found in wood-rotting basidiomycetes, other mechanisms are involved in aerobic degradation of N-heterocyclic compounds in bacteria and fungi (2, 26, 39). Key steps in the degradation of compounds containing structural elements also found in enrofloxacin, e.g., 3-carboxypyridine (nicotinic acid), 3,4-dihydroxypyridine, quinoline, 1*H*-4-oxoquinoline, and anthranilic acid, are catalyzed mostly by molybdenum-containing dehydrogenases, dioxygenases, or monooxygenases. Bauer and coworkers reported the degradation of 1*H*-3-hydroxy-4-oxoquinoline by *Pseudomonas putida* even via 2,4-dioxygenation, with concomitant elimination of carbon monoxide (5). However, FQs might not be readily accessible for such enzymes. Due to the fluorine substituent and the carbonyl as well as the carboxyl group, the heterocyclic core of enrofloxacin tends to be electron deficient. In addition, the high degree of substitution might prevent an enzymatic attack due to steric hindrance. Thus, the radical-based mechanisms, potentially employed by wood-rotting basidiomycetes, may provide the most suitable, if not the only, means to initiate degradation of such complex compounds. The ability of *G. striatum* to cleave the core structure of enrofloxacin also contradicts the reported apparent inability of brown rot fungi to degrade the aromatic components of lignin (15). Moreover, the reported growth of the brown rot fungus *Lentinus lepideus* on methoxylated aromatic compounds as sole sources of carbon is physiological evidence implying ring cleavage (11). Clearly, much more work is required to elucidate the reaction mechanism(s) utilized by brown rot fungi and to reveal their true potential in the degradation of lignocellulose and xenobiotics.

Ecological perspectives. In practice, animals undergoing antibacterial therapy will excrete a substantial fraction of an applied FQ as intact drug bound to feces; glucuronidation and sulfation of FQs cause only transient inactivation. Metabolites, characterized by an oxidized piperazine moiety, have been detected at small concentrations in urine and feces (27, 42). Because nonspecific binding restricts the mobility of FQs in the environment (13, 31, 34), manure (e.g., cattle dung) could serve as a relevant model ecosystem to study the fate of drugs, the more so because at least some of the known coprophilous basidiomycetes might also be able to degrade enrofloxacin.

Two such basidiomycetes were isolated from aged cattle dung by Wicklow and colleagues 2 decades ago (47, 48). These fungi appeared late on cattle dung, after various ascomycetes had consumed the more easily utilizable substrates. Both isolates, strain NRRL 6464 and a strain identified as *Cyathus stercoreus*, physiologically resembled wood-rotting fungi in showing a high activity in the degradation of lignocellulose in vitro (16, 48). Preliminary results from our laboratory indicate that *C. stercoreus* is able to degrade enrofloxacin (43). Therefore, under field conditions, the degradation of enrofloxacin might, in principle, proceed at the rate of decomposition of undigested plant polymers excreted by livestock animals or at that for the surrounding humus matrix.

Wood-rotting fungi, in degrading lignocellulose and other substances associated with such matrices, play an essential role in the global carbon cycle (6, 32), but very little is known about homologous taxa in agricultural soils and plant litter (41). So far, *G. striatum* has served as a model organism in proving that enrofloxacin (and, proven only very recently, ciprofloxacin [46]) is biodegradable. However, other, perhaps more appropriate, fungal species naturally present in dung and other relevant agricultural sites may have to be included to fully describe the natural degradation potential for FQs.

ACKNOWLEDGMENTS

We thank our colleagues at various chemistry departments at Bayer, namely, W. Hallenbach, R. Koch, R. Körmeling, U. Petersen, H. Rast, and R. Thomas, for providing the labeled and unlabeled standard compounds. Furthermore, we thank S. Ochtrop, A. Gerhardt, and J. Schneider, for excellent technical assistance.

REFERENCES

1. **Alef, K.** 1991. Methodenhandbuch Bodenmikrobiologie, p. 89. Ecomed Verlagsgesellschaft mbH, Landsberg, Germany.
2. **Andreoni, V., G. Baggi, and S. Bernasconi.** 1995. Microbial degradation of nitrogenous xenobiotics of environmental concern. Prog. Ind. Microbiol. **32:**1–36.
3. **Backa, S., J. Gierer, T. Reitberger, and T. Nilsson.** 1992. Hydroxyl radical activity in brown-rot fungi studied by a new chemiluminescence method. Holzforschung **46:**61–67.
4. **Barr, D. P., and S. D. Aust.** 1994. Pollutant degradation by white rot fungi, p. 49–72. *In* G. W. Ware (ed.), Reviews of environmental contamination and toxicology. Springer Verlag, New York, N.Y.
5. **Bauer, I., A. de Beyer, B. Tshisuaka, S. Fetzner, and F. Lingens.** 1994. A novel type of oxygenolytic ring cleavage: 2,4-oxygenation and decarbonylation of 1*H*-3-hydroxy-4-oxoquinaldine and 1*H*-3-hydroxy-4-oxoquinoline. FEMS Microbiol. Lett. **117:**299–304.
6. **Boominathan, K., and C. A. Reddy.** 1991. Fungal degradation of lignin: biotechnological applications, p. 763–822. *In* D. K. Arora, B. Rai, K. G. Mukerji, and G. R. Knudsen (ed.), Handbook of applied mycology, vol. 4. Marcel Dekker, Inc., New York, N.Y.
7. **Booth, D. M.** 1994. Enrofloxacin revisited. Vet. Med. **89:**744–753.
8. **Bumpus, J. A.** 1993. White rot fungi and their potential use in soil bioremediation processes. Soil Biochem. **8:**65–100.
9. **Bumpus, J. A., M. Tien, D. Wright, and S. D. Aust.** 1985. Oxidation of persistent environmental pollutants by a white rot fungus. Science **228:**1434–1436.
10. **Buswell, J. A.** 1991. Fungal degradation of lignin, p. 425–480. *In* D. K. Arora, B. Rai, K. G. Mukerji, and G. R. Knudsen (ed.), Handbook of applied mycology, vol. 1. Marcel Dekker, Inc., New York, N.Y.
11. **Collett, O.** 1992. Aromatic compounds as growth substrates for isolates of the brown-rot fungus *Lentinus lepideus* (Fr. ex. Fr.) Fr. Mater. Org. **27:**67–77.
12. **Domagala, J. M.** 1994. Structure-activity and structure-side-effect relationship for the quinolone antibacterials. J. Antimicrob. Chemother. **33:**685–706.
13. **Edlund, C., L. Lindqvist, and C. E. Nord.** 1988. Norfloxacin binds to human fecal material. Antimicrob. Agents Chemother. **32:**1869–1874.
14. **Eggert, C., U. Temp, J. F. D. Dean, and K.-E. L. Eriksson.** 1996. A fungal metabolite mediates degradation of non-phenolic lignin structures and synthetic lignin by laccase. FEBS Lett. **391:**144–148.
15. **Evans, C. S., M. V. Dutton, F. Guillen, and R. G. Veness.** 1994. Enzymes and small molecular mass agents involved with lignocellulose degradation. FEMS Microbiol. Rev. **13:**235–240.
16. **Freer, S. N., and R. W. Detroy.** 1982. Biological delignification of ^{14}C-labeled lignocelluloses by basidiomycetes: degradation and solubilization of the lignin and cellulose components. Mycologia **74:**943–951.
17. **Frost, A. J.** 1991. Antibiotics and animal production, p. 181–194. *In* J. B. Woolcock (ed.), Microbiology of animals and animal products. Elsevier, Amsterdam, The Netherlands.
18. **Greene, C. E., and S. C. Budsberg.** 1993. Veterinary use of quinolones, p. 473–488. *In* D. C. Hooper and J. S. Wolfson (ed.), Quinolone antimicrobial agents, 2nd ed. American Society for Microbiology, Washington, D.C.
19. **Halliwell, B., and J. M. Gutterridge.** 1989. Free radicals in biology and medicine, 2nd ed. Oxford University Press, Oxford, United Kingdom.
20. **Harper, D. B., and D. O'Hagan.** 1994. The fluorinated natural products. Nat. Products Rep. **11:**123–133.
21. **Hektoen, H., J. A. Berge, V. Hormazabal, and M. Yndestad.** 1995. Persistence of antibacterial agents in marine sediments. Aquaculture **133:**175–184.
22. **Hirano, T., H. Tanaka, and A. Enoki.** 1995. Extracellular substance from the brown-rot basidiomycete *Tyromyces palustris* that reduces molecular oxygen to hydroxyl radicals and ferric iron to ferrous iron. Mokuzai Gakkaishi **41:**334–341.
23. **Holzman, D.** 1995. Refractory chemical residues in soils may be safe. ASM News **61:**445–446.
24. **Hyde, S. M., and P. M. Wood.** 1996. Kinetic and antigenic similarities for cellobiose dehydrogenase from the brown rot fungus *Coniophora puteana* and the white rot fungus *Phanerochaete chrysosporium*. FEMS Microbiol. Lett. **145:**439–444.
25. **Joseleau, J.-P., S. Gharibian, J. Comtat, A. Lefebvre, and K. Ruel.** 1994. Indirect involvement of ligninolytic enzyme systems in cell wall degradation. FEMS Microbiol. Rev. **13:**255–264.
26. **Kaiser, J.-P., Y. Feng, and J.-M. Bollag.** 1996. Microbial metabolism of pyridine, quinoline, acridine, and their derivatives under aerobic and anaerobic conditions. Microbiol. Rev. **60:**483–498.
27. **Karabalut, N., and G. L. Drusano.** 1993. Pharmacokinetics of the quinolone antimicrobial agents, p. 195–223. *In* D. C. Hooper and J. S. Wolfson (ed.), Quinolone antimicrobial agents, 2nd ed. American Society for Microbiology, Washington, D.C.
28. **Kirk, T. K., R. Ibach, M. D. Mozuch, A. H. Conner, and T. L. Highley.** 1991. Characteristics of cotton cellulose depolymerized by a brown-rot fungus, by acid, or by chemical oxidants. Holzforschung **45:**239–244.
29. **Kleman-Leyer, K., E. Agosin, A. H. Conner, and T. K. Kirk.** 1992. Changes in molecular size distribution of cellulose during attack by white rot and brown rot fungi. Appl. Environ. Microbiol. **58:**1266–1270.
30. **Koenigs, J. W.** 1974. Hydrogen peroxide and iron: a proposed system for decomposition of wood by brown-rot basidiomycetes. Wood Fiber **6:**66–80.
31. **Marengo, J. R., R. A. Kok, K. O'Brien, R. R. Velagaletti, and J. M. Stamm.** 1997. Aerobic biodegradation of (^{14}C)-sarafloxacin hydrochloride in soil. Environ. Toxicol. Chem. **16:**462–471.
32. **Markham, P., and M. J. Bazin.** 1991. Decomposition of cellulose by fungi, p. 379–424. *In* D. K. Arora, B. Rai, K. G. Mukerji, and G. R. Knudsen (ed.), Handbook of applied mycology, vol. 1. Marcel Dekker, Inc., New York, N.Y.
33. **Martens, R., H.-G. Wetzstein, F. Zadrazil, M. Capelari, P. Hoffmann, and N. Schmeer.** 1996. Degradation of the fluoroquinolone enrofloxacin by wood-rotting fungi. Appl. Environ. Microbiol. **62:**4206–4209.
34. **Nowara, A., J. Burhenne, and M. Spiteller.** 1997. Binding of fluoroquinolone carboxylic acid derivatives to clay. J. Agric. Food Chem. **45:**1459–1463.
35. **Orth, A. B., and M. Tien.** 1995. Biotechnology of lignin degradation, p. 287–302. *In* K. Esser and P. A. Lemke (ed.), The mycota, vol. II. Genetics and biotechnology. Springer Verlag, Berlin, Germany.
36. **Ribbons, D. W., A. E. G. Cass, J. T. Rossiter, S. J. C. Taylor, M. P. Woodland, D. A. Widdowson, S. R. Williams, P. B. Baker, and R. E. Martin.** 1987. Biotransformation of fluoroaromatic compounds. J. Fluorine Chem. **37:**299–326.
37. **Ritschkoff, A.-C., M. Rättö, J. Buchert, and L. Viikari.** 1995. Effect of carbon source on the production of oxalic acid and hydrogen peroxide by brown-rot fungus *Poria placenta*. J. Biotechnol. **40:**179–186.
38. **Schlosser, D., R. Grey, and W. Fritsche.** 1997. Patterns of ligninolytic enzymes in *Trametes versicolor*. Distribution of extra- and intracellular enzyme activities during cultivation on glucose, wheat straw and beech wood. Appl. Microbiol. Biotechnol. **47:**412–418.
39. **Schwarz, G., and F. Lingens.** 1994. Bacterial degradation of N-heterocyclic compounds, p. 459–486. *In* C. Ratledge (ed.), Biochemistry of microbial

degradation. Kluwer Academic Publishers, Dordrecht, The Netherlands.
40. **Stalpers, J. A.** 1978. Identification of wood-inhabiting fungi in pure culture. Studies in mycology, no. 16. Centraalbureau voor Schimmelcultures, Baarn, The Netherlands.
41. **Thorn, G. R., C. A. Reddy, D. Harris, and E. A. Paul.** 1996. Isolation of saprophytic basidiomycetes from soil. Appl. Environ. Microbiol. **62:**4288–4292.
42. **Vancutsem, P. M., J. G. Babish, and W. S. Schwark.** 1990. The fluoroquinolone antimicrobials: structure, antimicrobial activity, pharmacokinetics, clinical use in domestic animals and toxicity. Cornell Vet. **80:**173–186.
43. **Wetzstein, H.-G.** Unpublished data.
44. **Wetzstein, H.-G., and A. de Jong.** 1996. In vitro bactericidal activity and postantibiotic effect of fluoroquinolones used in veterinary medicine. Compend. Contin. Educ. Pract. Vet. **18**(Suppl.)**:**S22–S29.
45. **Wetzstein, H.-G., H.-G. Rast, J. P. E. Anderson, J. Köster, and N. Schmeer.** 1996. In vitro degradation of the fluoroquinolone enrofloxacin by two species of wood-rot fungi, p. 414, abstr. Q-168. *In* Abstracts of the 96th General Meeting of the American Society for Microbiology 1996. American Society for Microbiology, Washington, D.C.
46. **Wetzstein, H.-G., N. Schmeer, A. Dalhoff, and W. Karl.** 1997. Degradation of the fluoroquinolone ciprofloxacin by the brown rot fungus *Gloeophyllum striatum* DSM 9592, p. 519, abstr. Q-388. *In* Abstracts of the 97th General Meeting of the American Society for Microbiology 1997. American Society for Microbiology, Washington, D.C.
47. **Wicklow, D. T.** 1992. The coprophilous fungal community: an experimental system, p. 715–728. *In* G. C. Carrol and D. T. Wicklow (ed.), The fungal community. Its organisation and role in the ecosystem, 2nd ed. Marcel Dekker, Inc., New York, N.Y.
48. **Wicklow, D. T., R. W. Detroy, and B. A. Jessee.** 1980. Decomposition of lignocellulose by *Cyathus stercoreus* (Schw.) de Toni NRRL 6473, a "white rot" fungus from cattle dung. Appl. Environ. Microbiol. **40:**169–170.
49. **Wolfson, J. S., and D. C. Hooper.** 1989. Fluoroquinolone antimicrobial agents. Clin. Microbiol. Rev. **2:**378–424.
50. **Wood, P. M.** 1994. Pathways for production of Fenton's reagent by wood-rotting fungi. FEMS Microbiol. Rev. **13:**313–320.
51. **World Health Organization.** 1995. Evaluation of certain veterinary drug residues in food. Forty-third report of the Joint FAO/WHO Expert Committee on Food Additives. WHO Tech. Rep. Ser. **855:**17–24.